CHEMISTRY OF MATERIALS
Article

Chem. Mater. **2010,** *22,* 3441–3450 3441
DOI:10.1021/cm100477v

Graphene/Polyurethane Nanocomposites for Improved Gas Barrier and Electrical Conductivity

Hyunwoo Kim, Yutaka Miura, and Christopher W. Macosko*

Department of Chemical Engineering and Materials Science, University of Minnesota, Minneapolis, Minnesota 55455-0331

Received February 15, 2010. Revised Manuscript Received April 30, 2010

Recently developed strategies for isolating single-layer carbon sheets from graphite have enabled production of electrically conductive, mechanically robust polymer nanocomposites with enhanced gas barrier performance at extremely low loading. In this article, we present processing, morphology, and properties of thermoplastic polyurethane (TPU) reinforced with exfoliated graphite. For the first time, we compare carbon sheets exfoliated from graphite oxide (GO) via two different processes: chemical modification (isocyanate treated GO, iGO) and thermal exfoliation (thermally reduced GO, TRG), and three different methods of dispersion: solvent blending, in situ polymerization, and melt compounding. Incorporation of as low as 0.5 wt % of TRG produced electrically conductive TPU. Up to a 10-fold increase in tensile stiffness and 90% decrease in nitrogen permeation of TPU were observed with only 3 wt % iGO, implying a high aspect ratio of exfoliated platelets. Real- and reciprocal-space morphological characterization indicated that solvent-based blending techniques more effectively distribute thin exfoliated sheets in the polymer matrix than melt processing. This observation is in good qualitative agreement with the dispersion level inferred from solid property enhancements. Although also processed in solvents, property increase via in situ polymerization was not as pronounced because of reduced hydrogen bonding in the TPU produced.

1. Introduction

Graphene, atomically thin two-dimensional sheets of carbon, has emerged as the subject of enormous interest because of its exceptional micromechanical and electron transport properties. Graphene has a high basal plane elastic modulus, $E \approx 1$ TPa;ultimate strength, $\sigma_{ultimate} \sim 130$ GPa; and room-temperature charge-carrier mobility, $\mu \approx 10\,000$ cm^2/V s.[1,2] Adding highly exfoliated carbon layers can significantly alter mechanical and electrical properties of polymers at extremely small loading.[3−6] Unlike carbon nanotubes that can provide similar mechanical and electrical benefits, these impermeable two-dimensional sheets can reduce gas permeability of host membranes.[5,6] Graphene can be derived directly from naturally occurring graphite via top-down methods such as mechanical cleavage[2] and liquid-phase exfoliation.[7,8] However, low yield (∼1 wt %) and difficult removal of surfactants can limit application of the top-down approaches. Even though bottom-up strategies have been proposed using chemical vapor deposition,[9] epitaxial graphitization,[10] or synthesis from aromatic carbons,[11] large-scale production is still far from realization. Moreover, the produced high-purity graphene sheets tend to stack into graphite or scroll into tubes[12−14] in order to minimize their surface energy.

Recently, two different strategies were reported that allow mass production of graphene-like layers from graphite oxide (GO). As illustrated in Scheme 1, covalently bonded oxygen groups on the surface of GO serve as sites for gas-producing thermal decomposition[15,16]

*Corresponding author. Tel.: (612) 625-0092. Fax: (612) 626-1686. E-mail: macosko@umn.edu.

(1) Lee, C.; Wei, X.; Kysar, J. W.; Hone, J. *Science* **2008**, *321*, 385–388.
(2) Novoselov, K. S.; Geim, A. K.; Morozov, S. V.; Jiang, D.; Zhang, Y.; Dubonos, S. V.; Grigorieva, I. V.; Firsov, A. A. *Science* **2004**, *306*, 666–669.
(3) Stankovich, S.; Dikin, D. A.; Dommett, G. H. B.; Kohlhaas, K. M.; Zimney, E. J.; Stach, E. A.; Piner, R. D.; Nguyen, S. T.; Ruoff, R. S. *Nature* **2006**, *442*, 282–286.
(4) Ramanathan, T.; Abdala, A. A.; Stankovich, S.; Dikin, D. A.; Herrera-Alonso, M.; Piner, R. D.; Adamson, D. H.; Schniepp, H. C.; Chen, X.; Ruoff, R. S.; Nguyen, S. T.; Aksay, I. A.; Prud'-Homme, R. K.; Brinson, L. C. *Nat. Nanotechnol.* **2008**, *3*, 327–331.
(5) Kim, H.; Macosko, C. W. *Macromolecules* **2008**, *41*, 3317–3327.
(6) Kim, H.; Macosko, C. W. *Polymer* **2009**, *50*, 3797–3809.
(7) Hernandez, Y.; Nicolosi, V.; Lotya, M.; Blighe, F. M.; Sun, Z.; De, S.; McGovern, I. T.; Holland, B.; Byrne, M.; Gun'Ko, Y. K.; Boland, J. J.; Niraj, P.; Duesberg, G.; Krishnamurthy, S.; Goodhue, R.; Hutchison, J.; Scardaci, V.; Ferrari, A. C.; Coleman, J. N. *Nat. Nanotechnol.* **2008**, *3*, 563–568.
(8) Lotya, M.; Hernandez, Y.; King, P. J.; Smith, R. J.; Nicolosi, V.; Karlsson, L. S.; Blighe, F. M.; De, S.; Wang, Z.; McGovern, I. T.; Duesberg, G. S.; Coleman, J. N. *J. Am. Chem. Soc.* **2009**, *131*, 3611–3620.
(9) Kim, K. S.; Zhao, Y.; Jang, H.; Lee, S. Y.; Kim, J. M.; Kim, K. S.; Ahn, J.-H.; Kim, P.; Choi, J.-Y.; Hong, B. H. *Nature* **2009**, *457*, 706–710.
(10) Emtsev, K. V.; Bostwick, A.; Horn, K.; Jobst, J.; Kellogg, G. L.; Ley, L.; McChesney, J. L.; Ohta, T.; Reshanov, S. A.; Roehrl, J.; Rotenberg, E.; Schmid, A. K.; Waldmann, D.; Weber, H. B.; Seyller, T. *Nat. Mater.* **2009**, *8*, 203–207.
(11) Zhi, L.; Muellen, K. *J. Mater. Chem.* **2008**, *18*, 1472–1484.
(12) Viculis, L. M.; Mack, J. J.; Kaner, R. B. *Science* **2003**, *299*, 1361.
(13) Li, Q.; Li, Z.; Chen, M.; Fang, Y. *Nano Lett.* **2009**, *9*, 2129–2132.
(14) Kalaitzidou, K.; Fukushima, H.; Miyagawa, H.; Drzal, L. T. *Polym. Eng. Sci.* **2007**, *47*, 1796–1803.
(15) Schniepp, H. C.; Li, J.-L.; McAllister, M. J.; Sai, H.; Herrera-Alonso, M.; Adamson, D. H.; Prud'homme, R. K.; Car, R.; Saville, D. A.; Aksay, I. A. *J. Phys. Chem. B* **2006**, *110*, 8535–8539.
(16) McAllister, M. J.; Li, J.-L.; Adamson, D. H.; Schniepp, H. C.; Abdala, A. A.; Liu, J.; Herrera-Alonso, M.; Milius, D. L.; Car, R.; Prud'homme, R. K.; Aksay, I. A. *Chem. Mater.* **2007**, *19*, 4396–4404.

Published on Web 05/17/2010

Scheme 1. Schematics of TPU/Graphene Composite Preparation Routes: (a) After Oxidizing Graphite in Concentrated Acids, Functionalized Graphene Layers Can Be Obtained via Either (b) Rapid Thermal Expansion (TRG, 2000 °C/min to 1050 °C in argon) or (c) Organic Modification with Isocyanate in DMF (iGO); (d) Graphite and TRG Can Be Incorporated into TPU via Melt-State Compounding; (e) Alternatively, Blending Can Take Place in DMF, Followed by Solvent Removal; (f) Composites Can Also Be Produced from Monomers Instead of Polymers Using In situ Polymerization[a]

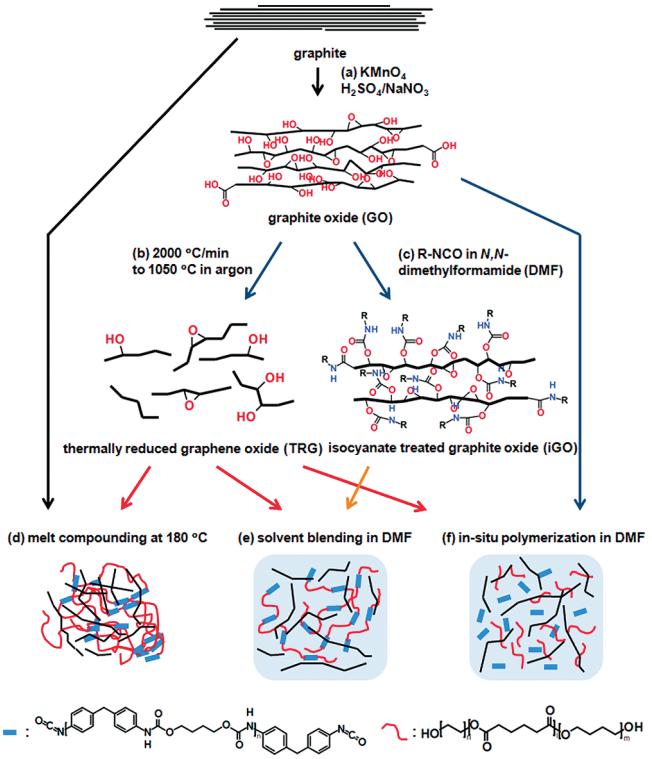

[a] Black lines represent graphitic reinforcements. TPU hard and soft segment are denoted by short blue blocks and thin red curves, respectively.

(Scheme 1b) or chemical functionalization[3,17] (Scheme 1c). CO_2 produced by rapidly heating (~2000 °C/min) GO up to 1050 °C pressurizes and mechanically splits apart GO stacks weakly bound by van der Waals forces.[16] Because of the enormous surface area (700−1500 m^2/g), surface polarity, and high electrical conductivity,[15] the resulting thermally reduced graphene oxide (TRG) sheets can be used to produce polymer composites with excellent mechanical, electrical, and thermal properties.[4−6] Deformation of the planar structure by oxidation and pyrolysis prevents restacking of layers, but reduces the ability of TRG to stiffen especially glassy polymers.[5,6] Stankovich and coworkers[3,17] showed that, in contrast to the starting GO, isocyanate-treated GO (iGO) readily forms a stable suspension in polar aprotic organic solvents enabling fabrication of completely exfoliated graphite/polymer nanocomposites via solvent blending. Electrical conduction of the graphitic sheets can be restored by in situ chemical reduction of GO with dimethylhydrazine,[18] leading to electrical percolation at as low as 0.1 vol %.[3]

We produced thermoplastic polyurethane (TPU) reinforced with these functionalized graphene materials. TPU is an elastomeric copolymer consisting of alternating hard and soft blocks which can phase separate. Because of melt processability and physical properties tunable over a wide range, TPU has been used for a variety of applications such as fibers, coatings, adhesives,[19] and biomimetic materials.[20] However, despite good deformability, low stiffness and tensile strength can limit its use in structural applications, especially for TPU with low hard block content. Water vapor and other gas permeability can be another drawback. The weak mechanical and gas barrier properties can be complemented by reinforcing the elastomeric matrix with rigid, impermeable nanofillers. For example, increased stiffness and toughness without compromising high extensibility,[21] enhanced shape memory,[22] and gas barrier performances[23] of TPU have been demonstrated by reinforcement with layered silicates and with carbon nanotubes. Graphene sheets are a promising alternative to these nanofillers, making electrically conductive, moisture barrier nanocomposite materials possible even at less than 1 wt % loading. Significantly enhanced tensile properties[24] and electrical percolation at 2 wt % TRG[25,26] have already been reported for a water-borne polyurethane.

GO, TRG, and iGO were incorporated into an ester-polyol based TPU elastomer (Avalon 70AE, Huntsman Polyurethanes) containing 25 wt % hard segment via melt intercalation, solvent mixing, and in situ polymerization. These are the 3 most commonly used methods for incorporation of the nanoscale reinforcements into polymers.[27,28] The schematics for each dispersion strategy are shown in Scheme 1. In melt intercalation (Scheme 1d), compounding took place above the melting point of TPU hard domain, which was mechanically assisted using extrusion.[29] Although this melt-state compounding is the most economically viable and environmentally friendly approach because it does not necessitate solvents, it is not a suitable option for matrices or inclusions that are prone to thermal degradation.

Solution mixing[21,30] (Scheme 1e) involves dispersing additive phase, dissolving matrix polymer in cosolvents,

(17) Stankovich, S.; Piner, R. D.; Nguyen, S. T.; Ruoff, R. S. *Carbon* **2006**, *44*, 3342–3347.
(18) Stankovich, S.; Dikin, D. A.; Piner, R. D.; Kohlhaas, K. A.; Kleinhammes, A.; Jia, Y.; Wu, Y.; Nguyen, S. T.; Ruoff, R. S. *Carbon* **2007**, *45*, 1558–1565.
(19) Woods, G. *The ICI Polyurethanes Book*; Wiley: New York, 1990.
(20) Lamda, N. M. K.; Woodhouse, K. A.; Cooper, S. L. *Polyurethanes in Biomedical Applications*; CRC Press: Boca Raton, FL, 1998.
(21) Liff, S. M.; Kumar, N.; McKinley, G. H. *Nat. Mater.* **2007**, *6*, 76–83.
(22) Koerner, H.; Price, G.; Pearce, N. A.; Alexander, M.; Vaia, R. A. *Nat. Mater.* **2004**, *3*, 115–120.
(23) Osman, M. A.; Mittal, V.; Morbidelli, M.; Suter, U. W. *Macromolecules* **2003**, *36*, 9851–9858.
(24) Lee, Y. R.; Raghu, A. V.; Jeong, H. M.; Kim, B. K. *Macromol. Chem. Phys.* **2009**, *210*, 1247–1254.
(25) Nguyen, D. A.; Lee, Y. R.; Raghu, A. V.; Jeong, H. M.; Shin, C. M.; Kim, B. K. *Polym. Int.* **2009**, *58*, 412–417.
(26) Raghu, A. V.; Lee, Y. R.; Jeong, H. M.; Shin, C. M. *Macromol. Chem. Phys.* **2008**, *209*, 2487–2493.
(27) Alexandre, M.; Dubois, P. *Mater. Sci. Eng., R* **2000**, *R28*, 1–63.
(28) Moniruzzaman, M.; Winey, K. I. *Macromolecules* **2006**, *39*, 5194–5205.
(29) Chavarria, F.; Paul, D. R. *Polymer* **2006**, *47*, 7760–7773.
(30) Finnigan, B.; Martin, D.; Halley, P.; Truss, R.; Campbell, K. *Polymer* **2004**, *45*, 2249–2260.

and recovering the composites via solvent evaporation or coagulation using nonsolvents. Although this approach generally leads to better particle dispersion than melt processing, slow solvent evaporation often induces particle reaggregation and commercialization is restricted by cost and environmental limitations of solvents. Because unmodified graphene has very limited solubility in most organic solvents,[7] functionalization of graphene is needed to improve the solubility.[17,31]

Alternatively, composites can be produced from monomers that can be in situ polymerized in the presence of dispersed nanoparticles (Scheme 1f).[32] Tien and Wei[32] and Pattanayak and Jana[33,34] reported that using layered silicates with reactive functional groups (−OH) can greatly improve particle dispersion and tensile strength as well as stiffness of the composites. Because TRG and GO have surface hydroxyls that can react with isocyanate (−NCO) groups, they may also serve as pseudo chain extenders for TPU. Successful covalent grafting of GO with long chain alkyl-chlorosilane,[35] amino,[36] and carboxylic[37] groups and in situ polymerization of a water-borne polyurethane with TRG[24] have been previously demonstrated.

In this article, we present processing, morphology, and properties of TPU/graphene nanocomposites. Unintercalated graphite and TRG were incorporated into TPU via melt intercalation. Solvent blending was also used to prepare TRG and iGO composites. TPU was in situ polymerized with GO or TRG using chain extension reaction with surface functional groups. Morphology of composites was characterized with transmission electron microscopy (TEM) and wide-angle X-ray diffraction (WAXD). Dispersion state of graphene inferred from TEM and WAXD was compared with enhancement in electrical, mechanical, and gas barrier properties of TPU.

2. Experimental Section

2.1. Materials. Avalon 70AE (Shore hardness: 70AE, density: 1.21 g/cm^3) was provided by Huntsman Polyurethanes. The highest hard segment dissociation temperature is ∼150 °C as measured by differential scanning calorimetry (Q1000, TA Instruments). Zero-shear melt viscosity at 180 °C by rotational rheometry (ARES, TA Instruments) is ∼600 Pa·s. Ester-based polyol (Daltorez P765, Huntsman Polyurethanes, molecular weight M_w = 2200 g/mol), 4,4′-methylene diphenyl diisocyanate (MDI, Rubinate 44, Huntsman Polyurethanes) and 1,4-butanediol (BDO, Sigma Aldrich) were used for in situ polymerization.

Flake graphite (surface enhanced, grade # 3775) was purchased from Asbury Carbons and the thermally reduced graphene oxide (TRG) was provided by Vorbeck Materials. Synthesis of TRG is described elsewhere.[15] The surface area of as-received graphite and TRG estimated by Brunauer, Emmett and Teller (BET)[38] N_2 adsorption (Autosorb-1, Quantachrome) are 29 and ∼800 m^2/g, respectively.[6] GO was produced from high purity graphite powders (SP-1 graphite, Bay Carbon, average particle diameter: 30 μm) following Hummers and Offeman's method.[39] Briefly explaining the synthesis procedure, 5 g of SP-1 graphite in a round-bottom flask was stirred in a mixture of concentrated sulfuric acid (95−98%, 80 mL) and sodium nitrate (2.5 g, Sigma-Aldrich). After adding 20 g of potassium permanganate (Sigma-Aldrich), temperature of the reaction mixture was maintained at ∼35 °C in an ice bath. When vigorous effervescence ceased, GO paste was gradually diluted in deionized (DI) water (6 L). The diluted solution was treated with 30% hydrogen peroxide and 10% hydrochloric acid to reduce insoluble ions[40] and then filtered through a fritted glass filter. The product was repeatedly washed with DI water until pH of the filtrate became ∼6. GO was dried in a vacuum oven at 45 °C before use. After dehydration, GO (2 g) was treated with 80 mmol of phenyl isocyanate (Ph-iGO) or acetylphenyl isocyanate (AcPh-iGO) for iGO synthesis[17] in anhydrous *N,N*-dimethylformamide (DMF, 200 mL) under N_2 for 48 h. All reagents were obtained from Sigma Aldrich and used as received. After reaction, iGO was precipitated by adding into methylene chloride (1 L).

2.2. Characterization of GO Derivatives. Elemental analysis results for GO, TRG, and iGO were obtained from Atlantic Microlab (Norcross, GA). X-ray photoelectron spectroscopy (XPS, see Supporting Information 1) was also used to evaluate atomic compositions in the graphitic carbons. Dimensions of GO and TRG on a freshly cleaved mica substrate (grade V1, Ted Pella) were estimated with contact-mode atomic force microscopy (AFM, Proximal Nanoprobe Scanning Probe Nanoscope, Digital Instruments). Particles were deposited from suspensions of GO in DI water or TRG in tetrahydrofuran (THF) prepared at 10 μg/mL by mild stirring for ∼3 weeks (GO) and ∼2 days (TRG). Combined small- and wide-angle X-ray scattering (SAXSESS, Anton Paar) was employed to measure the layer expansion after chemical intercalation of graphite. Detailed procedures for the contact-mode AFM and X-ray scattering are illustrated elsewhere.[5] Graphite and its derivatives were also characterized with confocal Raman (see Supporting Information 2) and Fourier transform infrared (FTIR, see Supporting Information 3) spectroscopy.

2.3. Composite Processing. Melt compounding, solvent blending, and in situ polymerization were used to prepare TPU/graphene composites. Cryo-pulverized (Spex 6700 Freezer/Mill) TPU powders were dried with graphite or TRG in a vacuum at 50 °C for 24 h prior to melt processing. They were fed into a recirculating, conical twin-screw extruder (Microcompounder, DACA Instruments) at 180 °C and blended under dry N_2 for 6 min at the screw speed of 360 rpm. Melt-blended samples were further processed into ∼0.1 mm thick films by hot pressing (140 kPa for 2 min) at 180 °C.

Dispersion of TRG, iGO, and GO into TPU was also conducted in DMF via either solvent blending or in situ polymerization. In solvent mixing, graphitic additives (10−60 mg) were dispersed in DMF (20 mL) and stirred with a magnetic bar for 2 days (TRG) or 20 days (iGO). Dry TPU powders (∼2 g) were then added to the suspensions and stirred for additional 2 days.

(31) Stankovich, S.; Piner, R. D.; Chen, X.; Wu, N.; Nguyen, S. T.; Ruoff, R. S. *J. Mater. Chem.* **2006**, *16*, 155–158.
(32) Tien, Y. I.; Wei, K. H. *Macromolecules* **2001**, *34*, 9045–9052.
(33) Pattanayak, A.; Jana, S. C. *Polymer* **2005**, *46*, 3275–3288.
(34) Pattanayak, A.; Jana, S. C. *Polymer* **2005**, *46*, 3394–3406.
(35) Matsuo, Y.; Tabata, T.; Fukunaga, T.; Fukutsuka, T.; Sugie, Y. *Carbon* **2005**, *43*, 2875–2882.
(36) Herrera-Alonso, M.; Abdala, A. A.; McAllister, M. J.; Aksay, I. A.; Prud'homme, R. K. *Langmuir* **2007**, *23*, 10644–10649.
(37) Salavagione, H. J.; Gomez, M. A.; Martinez, G. *Macromolecules* **2009**, *42*, 6331–6334.
(38) Brunauer, S.; Emmett, P. H.; Teller, E. *J. Am. Chem. Soc.* **1938**, *60*, 309–19.
(39) Hummers, W. S., Jr.; Offeman, R. E. *J. Am. Chem. Soc.* **1958**, *80*, 1339.
(40) Titelman, G. I.; Gelman, V.; Bron, S.; Khalfin, R. L.; Cohen, Y.; Bianco-Peled, H. *Carbon* **2005**, *43*, 641–649.

For in situ polymerization, polymerization and blending were carried out in DMF rather than in bulk-phase since a rapid viscosity increase with polymerization made mixing difficult. Polyol and BDO were dehydrated at 70 °C under a vacuum for 24 h and MDI was also vacuum-dried at 30 °C for 2 h. Prepolymers were synthesized by mixing dry polyol and MDI at 95 °C under N_2 for 4 h. TRG or GO in anhydrous DMF (~180 mL) stirred for 1 day (TRG) or 7 days (GO) was poured into the prepolymer at 45 °C and blended further for at least 6 h (TRG) or 24 h (GO). The chain extender BDO was added to the solution and stirring continued for additional 24−72 h. Weight and molar ratios of each component for in situ polymerization can be found in Supporting Information 4 along with average molecular weights of the products determined by size exclusion chromatography (SEC). Polymerized composites were recovered from DMF by coagulating in methanol with vigorous mixing. After being dried, products were redispersed in DMF. DMF solutions containing solvent-blended or in situ polymerized samples were cast on a heated glass plate (~55 °C). DMF removal from the cast films continued for 48 h in a vacuum oven at 50 °C before characterization. Temperatures were kept low for both solvent blending and in situ polymerization because GO and its derivatives decompose[15,18] even below 100 °C.

2.4. Composite Characterization. Dispersion of graphene in TPU was examined with TEM imaging and WAXD. Composites were cryo-microtomed (Leica Ultracut) with a diamond knife at −90 °C into ~100 nm thick slices and placed on 400-mesh Cu TEM grids. Thin film samples were embedded in an epoxy matrix (TRA-BOND 2115, Tra-Con) prior to the microtome. Bright field TEM micrographs were obtained with JEOL 1210 at an accelerating voltage of 120 kV. WAXD intensity was collected in a transmission mode with a Bruker-AXS microdiffractometer and CuKα radiation (45 kV and 40 mA). X-rays were directed to ~3 mm wide films both in the thickness and in the transverse direction. Scattering intensity I as a weighted sum ($2I_{transverse} + I_{thickness}$) after normalization based on the scattering volume is reported.

Electrical conductivity was measured with an 11-point dc surface resistance meter (PRS-801, Prostat). Measurements were repeated on 3−4 different areas of the composite films to ensure sample uniformity and their geometric averages are reported. Tensile deformation was applied to 4 mm wide composite films at a rate of 5×10^{-4} s^{-1} with Rheometrics Solids Analyzer II to evaluate static Young's moduli, E. Tests were conducted on 3−4 samples. Gas permeability tests were carried out using a constant volume-variable pressure apparatus[41,42] at 35 °C on disks (diameter: 4.2 cm) cut from composite films. N_2 flow was fed to one side of the specimen at 1 atm and temporal pressure change in the opposite, evacuated side was recorded.

To characterize the extent of interurethane hydrogen bonding interaction in the TPU matrix, FTIR spectroscopy in an attenuated total reflection (ATR) mode was employed. After vacuum dehydrating at room temperature for 24 h, TPU or composite films were pressed against ZnSe crystal of a Nicolet Magna-IR 750 spectrometer and spectra averaged over 40 ATR scans were taken from 2−3 different sample locations. Infrared (IR) transmittance in the range of 1800−1650 cm^{-1} (stretching of carbonyl groups)[43] was baseline subtracted using a linear baseline drawn from 1800 to 2800 cm^{-1}, where no noticeable absorption was detected.

Table 1. Atomic Concentrations in Graphitic Derivatives from Elemental Analysis and XPS

	elemental analysis				XPS			
material	C	O	N	H	C	O	N	S
graphite	N/A				~ 100			
GO	50	29		21	69	30		1
Ph-iGO	53	20	2	25	72	27	1	
TRG	92	4		4	82	18		

3. Results and Discussion

Graphite oxide and its derivatives were characterized using elemental analysis, X-ray scattering, solubility tests, and AFM. After incorporation into TPU via melt- and solvent-state blending and in situ polymerization, the dispersion state of graphene was analyzed with real- and reciprocal-space morphological characterization. TPU/graphene composites were tested for electrical conductivity, mechanical properties, and N_2 permeation. For the weight to volume fraction conversion, densities of graphitic reinforcements were all assumed to be 2.28 g/cm^3, which was calculated from the unit-cell dimensions of perfectly crystalline graphite.[5]

3.1. Graphene Characterization. *3.1.1. Elemental Analysis.* Atomic compositions in the graphitic carbons from elemental analysis are compared with those from XPS in Table 1. XPS survey scans and high-resolution C_{1s} scans of graphite, GO, Ph-iGO. and TRG can be found in Supporting Information 1. Note that XPS cannot detect hydrogen atoms. After oxidation, oxygen concentration in graphite increased up to 30 mol %. The asymmetric C_{1s} spectrum of GO (Supporting Information 1) also suggests formation of carbon−oxygen bonds. Both XPS and elemental analysis show a reduction in oxygen, indicating that thermal exfoliation led to partial reduction of GO. In addition to carbon and oxygen, sulfur was detected from the surface of GO, which may be traced to sulfate ions physically trapped in closed pores or covalently esterified with surface hydroxyls.[40] Nitrogen detected from Ph-iGO is from carbamate or amide groups in iGO, which substantiates the surface functionalization with isocyanate. Covalent incorporation of oxygen on GO and isocyanate groups on iGO was also confirmed with Raman spectroscopy (Supporting Information 2) and FTIR (Supporting Information 3).

3.1.2. X-ray Scattering. Functionalization also modifies the average intergallery distance of stacked graphene. A sharp reflection at $2\theta = 26.4°$ in the X-ray scattering pattern of pristine graphite (Figure 1) originates from the interlayer (002) spacing ($d = 0.34$ nm). Upon oxidation, neighboring layers are ~0.70 nm apart ($2\theta = 12.7°$) because of the intercalation by oxygen groups and moisture.[44] As well as the shift to lower angle, peak broadening takes place because of the disorder introduced by reduced average crystalline

(41) Pye, D. G.; Hoehn, H. H.; Panar, M. *J. Appl. Polym. Sci.* **1976**, *20*, 1921–31.
(42) Jeong, H.-K.; Krych, W.; Ramanan, H.; Nair, S.; Marand, E.; Tsapatsis, M. *Chem. Mater.* **2004**, *16*, 3838–3845.
(43) Cooper, S. L.; Seymour, R. W.; Estes, G. M. *Macromolecules* **1970**, *3*, 579–83.
(44) Hontoria-Lucas, C.; Lopez-Peinado, A. J.; Lopez-Gonzalez, J. d. D.; Rojas-Cervantes, M. L.; Martin-Aranda, R. M. *Carbon* **1995**, *33*, 1585–1592.

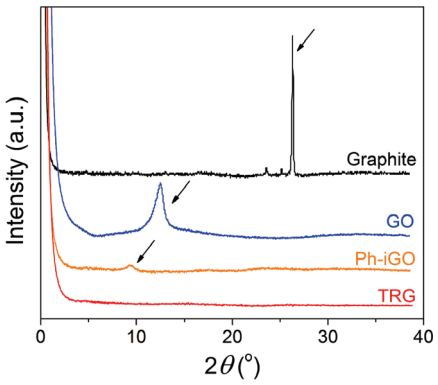

Figure 1. Combined small- and wide-angle X-ray diffractograms of graphite, GO, Ph-iGO, and TRG. Profiles were vertically shifted for clarity. Scattering reflections from the layered spacing of graphitic carbons are marked by arrows.

size. Treating with phenyl isocyanate expands the interlayer spacing of GO to $d = 0.95$ nm ($2\theta = 9.3°$); GO is separated by bulkier isocyanate moieties. In the scattering intensity profile of TRG, characteristic reflections are absent, implying complete exfoliation via superheating of GO.[15]

3.1.3. Solution Properties. Functionalization alters surface properties of graphene improving its solubility in organic solvents.[17] GO and Ph-iGO dispersions (1 mg/mL) in DI water and THF are shown in Figure 2a. Strong hydrophilic character of GO[45] can be inferred from its good dispersibility in water, whereas significant precipitation was observed in THF. GO treated with isocyanate can be well suspended even in a relatively nonpolar, aprotic medium such as THF. For Ph-iGO, THF turned out to be a better solvent than water, which signifies inversion in surface properties. Both materials formed fairly good dispersions in DMF (not shown here).

3.1.4. Contact-Mode AFM. Contact-mode AFM reveals that the typical lateral size of GO is on the order of micrometers (Figure 2b). The diameter of TRG, a few hundred nanometers, is substantially smaller. Considering the size of the parent graphite material that TRG was produced from, 45 μm,[15] significant size reduction during oxidation[46] and pyrolysis is evident. From the differences in step heights in the height profile of GO (the inset in Figure 2b), the thickness of a single GO sheet is ~1 nm, in agreement with estimates found in literature.[17] The difference from the interlamellar spacing of GO determined by X-ray diffraction, ~ 0.7 nm, may stem from surface water absorption. The apparent thickness of isolated TRG layers, ~1.8 nm, falls within the estimates by Schniepp and co-workers.[15] The vertical distance between the crest and the trough in the wrinkled sheets may contribute to the higher apparent thickness.

3.2. Composite Characterization. *3.2.1. Molecular Weights of TPU and Composites.* Polystyrene-calibrated weight (M_w) and number (M_n) average molecular weight of Avalon 70AE determined by SEC are 96 000 and 55 000 g/mol respectively with polydispersity index (PDI) of 1.7. After melt extrusion, molecular weight of Avalon 70AE was slightly reduced (M_w = 85 000 g/mol) perhaps due to some thermal degradation of polyurethane[47] during processing at 180 °C. M_w, M_n and PDI of in situ polymerized TPU are summarized in Supporting Information 4. M_w of TPU polymerized with GO or TRG varies from 28 000 to 155 000 g/mol. This variation may be caused by isocyanate consumption by oxygen groups on graphene, and particle inclusion in TPU samples separated from the composites, as discussed in Supporting Information 4. However, the variation in molecular weight does not appear to affect physical properties of the TPU (see Supporting Information 6 and 8).

3.2.2. Morphological Characterization. Real- and reciprocal-space morphological information of TPU composites was obtained using TEM (Figure 3) and WAXD (Figure 4). Melt-blended graphite composites show a thick tactoid-like structure in TEM (Figure 3a) and a sharp reflection at 2θ = 26.4° in WAXD. This suggests that without any exfoliation treatment graphite cannot be split into thin carbon layers via melt compounding. On the other hand, thin sheets of TRG blended under the same condition are homogenously distributed in Figure 3b even at lower particle concentration. Exfoliated morphology can also be inferred from its WAXD (Figure 4): no scattering for $2\theta > 3.5°$. WAXD patterns of solvent-blended and in situ polymerized TRG composites (not shown) also lack reflections from layered nanoparticles. However, TEM imaging does reveal differences in TRG structure dispersed via different dispersion routes. In contrast to the randomly oriented, curved thin sheets seen in solvent-mixed or in situ polymerized samples (Figure 3d,f), melt-compounded TRG appears more oriented with some stacking (Figure 3c). The higher matrix viscosity in the melt state and the flow fields associated with the extrusion process may result in these subtle morphological differences, which are not captured with WAXD. Scrolling into the tubular shape, which was commonly found from isolated thin carbon sheets,[12−14] was not observed.

Surface modification with isocyanate also led to GO sheets that can be well-separated after solvent mixing (Figure 3g). Nonetheless, in higher magnification (Figure 3h), layered stacks of a few iGO sheets can be also viewed. This type of morphology can be described as "intercalated" as suggested by the broad reflections centered at $2\theta \approx 4-7°$ in the WAXD (see the inset in Figure 4). It should be noted that GO sheets still maintain same layered structure after being treated with isocyanate, whereas rapid pyrolysis of GO completely exfoliates layers (see Figure 1). Medium viscosity (zero shear viscosity, $\eta_0 \approx 1$ mPa s (DMF) versus ~600 Pa s (TPU melt at 180 °C)) implies that particles will experience significantly weaker stress during blending in solution than in melt processing. Furthermore, if particle−matrix attraction cannot compete with particle−particle interaction, particles can aggregate rapidly during the relatively slow solvent evaporation required for film formation. Interestingly, GO particles that were in situ polymerized with TPU appear more

(45) Wen, X.; Garland, C. W.; Hwa, T.; Kardar, M.; Kokufuta, E.; Li, Y.; Orkisz, M.; Tanaka, T. *Nature* **1992**, *355*, 426–428.
(46) Li, J.-L.; Kudin, K. N.; McAllister, M. J.; Prud'homme, R. K.; Aksay, I. A.; Car, R. *Phys. Rev. Lett.* **2006**, *96*, 176101/1–176101/4.
(47) Yang, W. P.; Macosko, C. W.; Wellinghoff, S. T. *Polymer* **1986**, *27*, 1235–40.

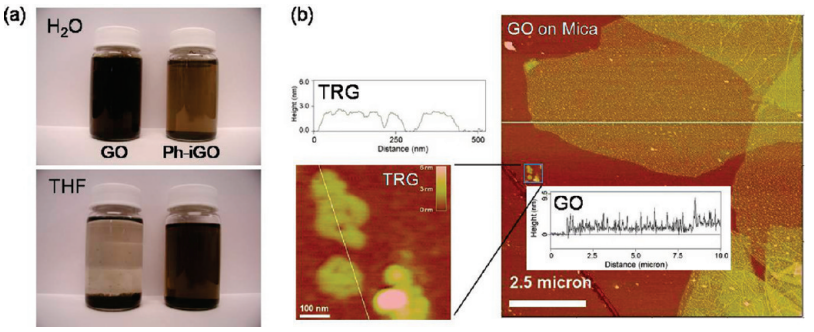

Figure 2. (a) GO and Ph-iGO suspensions in DI water and in THF (1 mg/mL) 4 h after ultrasonication for 1 h. (b) Contact-mode AFM scans of GO and TRG on mica substrates and their height profiles (insets) along the straight white lines.

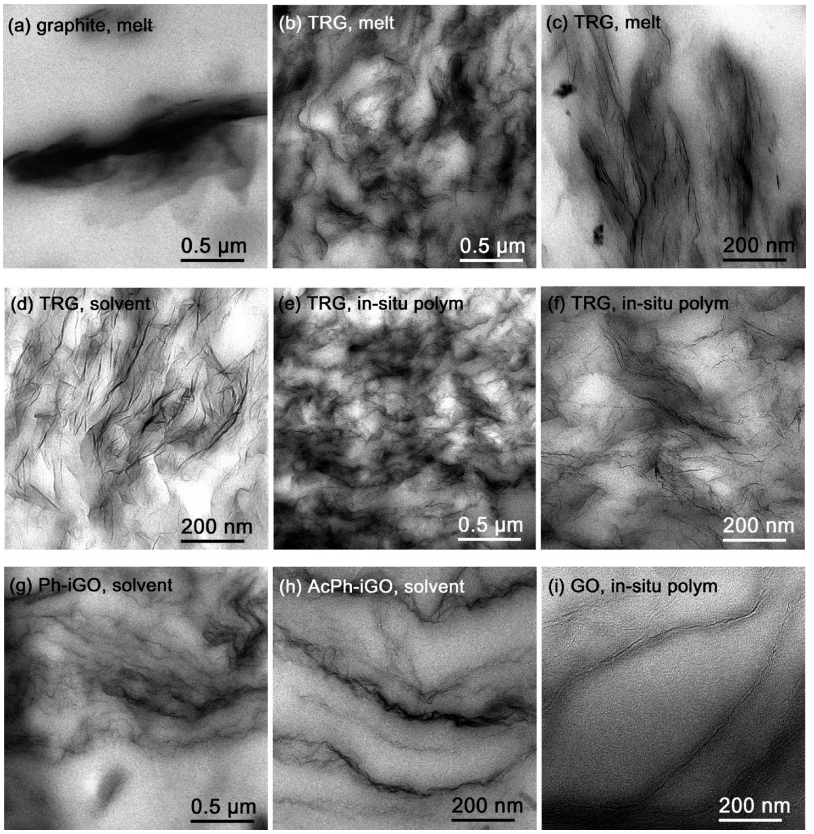

Figure 3. TEM micrographs of TPU with (a) 5 wt % (2.7 vol %) graphite, (b, c) melt-blended, (d) solvent-mixed, (e, f) in situ polymerized ~3 wt % (1.6 vol %) TRG, (g) solvent-mixed 3 wt % (1.6 vol %) Ph-iGO, (h) AcPh-iGO, and (i) in situ polymerized 2.8 wt % (1.5 vol %) GO.

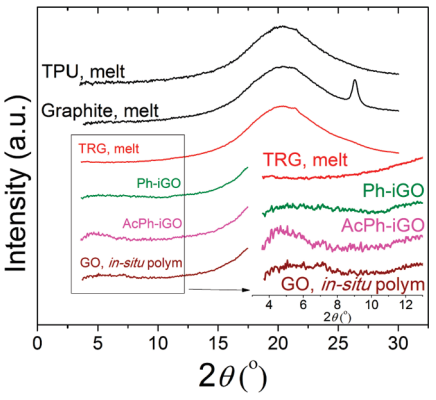

Figure 4. WAXD profiles of TPU composites. The inserts are WAXD patterns in $2\theta = 3.5-13°$ for melt-blended TRG, solvent-blended Ph-iGO, AcPh-iGO, and in situ polymerized GO composites.

extended and interconnected (Figure 3i). Functionalization with TPU chains may improve chemical affinity with the matrix, which should stretch out GO sheets as Hirata et al.[48] noted. Moreover, reaction of surface −OH groups by TPU terminated at each end with −NCO groups can result in particle bridging,[36] which can pillar graphene sheets together and thus increase their persistence length.

3.2.3. Composite Properties. Electrical, mechanical, and gas barrier properties of polymers can be dramatically influenced by graphene addition. In this section, we discuss improved physical properties of TPU reinforced with graphene.

(48) Hirata, M.; Gotou, T.; Horiuchi, S.; Fujiwara, M.; Ohba, M. *Carbon* **2004**, *42*, 2929–2937.

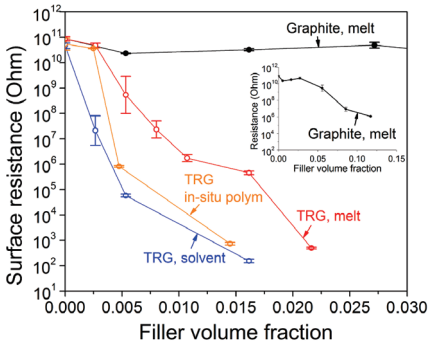

Figure 5. dc surface resistance of melt-blended graphite/TPU composites (closed symbols, also in inset) and melt-blended, solution-mixed, and in situ polymerized TRG/TPU composites (open symbols).

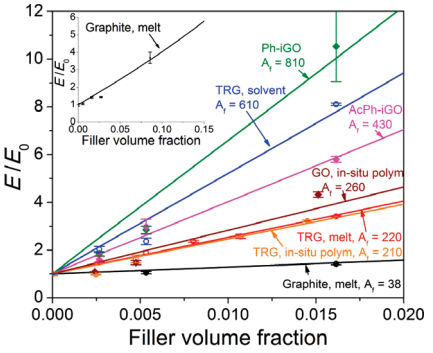

Figure 6. Young's moduli E of graphene/TPU composites normalized by matrix modulus E_0. Modulus data for melt-blended graphite composites are reproduced in the inset. Straight lines are predictions based on the Mori−Tanaka theory.[52]

3.2.3.1. Electrical Conductivity. Figure 5 shows the dc surface resistance of TPU containing graphite and TRG. Both graphite and TRG effectively increased electrical conductivity (reduced resistance), but they differ greatly in the onset concentration for electrical percolation (>2.7 vol% for untreated graphite versus <0.5 vol % for TRG). Conductivity measurements indicate that the average particle aspect ratio, A_f (ratio of diameter to thickness) of TRG is considerably greater than that of graphite since for randomly oriented disks, the percolation threshold is inversely proportional to A_f.[5] Among the TRG composites, conductivity of in situ polymerized and solvent-blended samples is higher than melt-blended ones at the same filler volume fraction. The resistance decrease takes place at even <0.3 vol % TRG in the case of solvent-mixed samples, whereas it requires >0.5 vol % for melt intercalation. This trend agrees with the TEM observation which indicated melt blending leads to platelet reaggregation. Particle attrition may also take place during melt extrusion, reducing the lateral size of TRG. Although processed with solvents, the percolation threshold of in situ polymerized composites is slightly greater, between 0.3 and 0.5 vol %. Covalently grafted TPU chains on TRG surface may hinder direct contacts between platelets, and reduce effective particle aspect ratios.[49] Note that there are no data for GO or iGO in Figure 5. They showed no decrease in surface resistance due to loss of electrical conductivity after graphite oxidation.[18] Graphite oxide can be chemically or thermally reduced[50] to restore electrical conductivity. However, chemical reduction must be conducted in a solution state in the presence of the matrix polymer to circumvent rapid reaggregation of reduced graphite oxide.[3] Electrophilic atoms in polyurethane can react with typical reducing agents such as hydrazine.[51]

3.2.3.2. Mechanical Properties. Reinforcement with graphene sheets also greatly enhances stiffness of polymers as shown in Figure 6. A list of tabulated raw modulus data is provided in Supporting Information 5. With a few exceptions, standard deviation is less than 10% of the modulus indicating reproducibility of measurements. A 250% increase in tensile modulus of TPU was observed at 9 vol % of graphite, whereas similar or even greater improvements were obtained by adding only 1.6 vol % (3 wt %) TRG or iGO. Higher stiffening efficiency of exfoliated graphite can be attributed to higher particle A_f. Effective medium theories such as one by Mori and Tanaka[52] for tensile stiffness of composites filled with rigid ellipsoidal inclusions can be used to quantify the extent of dispersion (e.g., A_f) from modulus measurements.[5,6,53] Using the analytical forms derived by Tandon and Weng[54] and experimentally or theoretically determined material parameters, A_f values of exfoliated carbon sheets were estimated so that they best fit the modulus increase as a function of filler volume fraction. For formulas and parameters used, see Supporting Information 7. Solvent-dispersed TRG and Ph-iGO are mechanically equivalent to flat rigid disks (E = 1 TPa) with A_f of ∼600 and ∼800, whereas A_f of untreated graphite is only 38. TRG dispersed via solvent blending appears to more effectively increase the modulus of TPU than TRG dispersed via melt processing (A_f = 220). Particle reaggregation and size reduction during melt extrusion may result in less stiffness increase, thus smaller A_f from modulus modeling. However, modulus increase by TRG incorporated via in situ polymerization is not as pronounced despite what appears to be good dispersion by TEM (compare Figure 3f to 3d). It is also worth mentioning that good elongation of TPU could be retained after graphene addition (see Supporting Information 8). In fact, incorporating small amounts (0.5−1.0 wt %) of TRG or GO improved tensile strength of in situ polymerized TPU significantly.

It should be noted that the aspect ratio A_f of iGO from modulus modeling (400−800) is far smaller than the highest possible A_f of isolated GO sheets estimated from AFM analysis (∼10 000, Figure 2b). Although particle attrition may play a role, iGO layers are mainly dispersed as highly curved stacks intercalated by polymer, see

(49) Wang, D. H.; Arlen, M. J.; Baek, J.-B.; Vaia, R. A.; Tan, L.-S. *Macromolecules* **2007**, *40*, 6100–6111.
(50) Eda, G.; Fanchini, G.; Chhowalla, M. *Nat. Nanotechnol.* **2008**, *3*, 270–274.
(51) Zalan, Z.; Lazar, L.; Fueloep, F. *Curr. Org. Chem.* **2005**, *9*, 357–376.
(52) Mori, T.; Tanaka, K. *Acta Metall.* **1973**, *21*, 571–574.
(53) Sheng, N.; Boyce, M. C.; Parks, D. M.; Rutledge, G. C.; Abes, J. I.; Cohen, R. E. *Polymer* **2004**, *45*, 487–506.
(54) Tandon, G. P.; Weng, G. J. *Polym. Compos.* **1984**, *5*, 327–333.

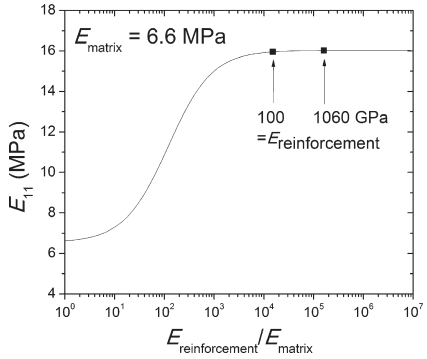

Figure 7. Transverse tensile modulus E_{11} predicted by the Mori−Tanaka theory for elastomeric (E = 6.6 MPa) polymer composites reinforced with 1 vol % A_f = 200 ellipsoids. Mori−Tanaka predicts that E_{11} remains nearly unaffected even when the in-plane stiffness of the ellipsoids decreases from 1060 to 100 GPa.

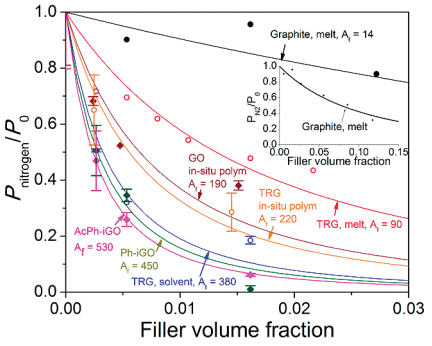

Figure 8. N_2 permeability, $P_{nitrogen}$, of TPU composites normalized by permeability P_0 of unfilled TPU. Permeability data for graphite composites are reproduced in the inset. Solid curves are predictions based on Lape et al.[58]

Figure 3g,h. Brune and Bicerano[55] argued that these stacks will have significantly diminished modulus and A_f compared with isolated sheets. Also, as Schaefer and Justice[56] pointed out for carbon nanotube/polymer composites, because of their high flexibility, quantification of graphene dispersion from modulus modeling rather reflects a local persistence length of the curved layers.

We previously reported surprisingly low modulus increase when TRG was added to rigid glassy polymers.[5,6] As shown in Supporting Information 6, we see similar modest improvements in modulus for TPU below the soft segment glass transition temperature, $T_{g,\,soft}$, whereas above $T_{g,\,soft}$ modulus nearly doubled for as little as 0.5 wt % solvent-blended TRG. We attributed this diminished reinforcing efficacy for glassy polymers to defects in the sheet structure formed by oxidation and pyrolysis, which can possibly reduce effective in-plane tensile stiffness of graphene from 1 TPa to even less than 100 GPa.[5] Nanoindentation study also revealed stiffness of chemically reduced GO can be as low as ~250 GPa.[57] However, this reduction in graphene stiffness has only minimal influence for elastomers. In Figure 7, transverse modulus E_{11} of TPU (E_{matrix} = 6.6 MPa) filled with perfectly aligned, rigid ellipsoids (A_f = 200, volume fraction = 0.01) is predicted as a function of the ratio between reinforcement $E_{reinforcement}$ and matrix E_{matrix} stiffness, using the Mori-Tanaka model and material parameters provided in Supporting Information 7. It suggests that there will be no additional gain in E_{11} when graphene stiffness is greater than ~100 GPa due to limited interfacial load transfer.[53] Therefore, possible sheet weakening down to $E_{reinforcement}$ = 100 GPa by defect-like structures will not appreciably decline the stiffening performance for elastomers.

3.2.3.3. Gas Barrier Properties. N_2 permeability, $P_{nitrogen}$, of TPU films filled with graphitic platelets at 35 °C is summarized in Figure 8. N_2 permeation is remarkably reduced demonstrating that exfoliated carbon sheets can be diffusion barriers in polymeric membranes. Dispersion state of graphene can be inferred from the decrease in gas permeability. $P_{nitrogen}$ versus volume fraction of graphene was fitted with the gas permeation model of Lape and co-workers varying A_f as an adjustable parameter.[58] The model used assumes monodisperse flakes all aligned to the polymer film but arrayed randomly. The 90% decrease in $P_{nitrogen}$ with 1.6 vol % (3 wt %) iGO is comparable with what can be achieved with unidirectionally aligned A_f = 400−500 flat impermeable disks, corroborating high aspect ratio of exfoliated carbon sheets. Layer misalignment would significantly undercut the barrier enhancement.[59] Thus, the actual particle A_f may be even greater than 400−500. Note that 3 wt % (1.6 vol %) of Ph-iGO leads to a remarkable 80 fold decrease in $P_{nitrogen}$. Because the barrier performance of two-dimensional platelets is determined only by particle aspect ratio, not by the micromechanics of sheets, iGO with larger diameter can be more advantageous for minimizing gas permeation. Moreover, disklike particles tend to adopt parallel orientation in nematic transition as the shape anisotropy or particle concentration grows.[60] Note that similar to the modulus results, in situ polymerized TRG is not as effective as solvent-blended TRG in reducing gas permeability.

3.2.4. FTIR and Solvent Extraction of TPU Composites. Despite similar dispersion levels of TRG (TEM, Figure 3d,f), in situ polymerization did not improve mechanical and gas barrier properties as significantly as solvent blending. This may be explained by reduced hydrogen bonding among urethane groups in TPU polymerized in the presence of functionalized graphene. ATR-FTIR spectrum (Figure 9) of TPU and its composites has at least two distinguished bands: a main peak centered at 1730 and a relatively small shoulder around 1715 cm^{-1}. The peak at 1730 cm^{-1} is associated with −C═O groups that are "free" (non-hydrogen bonded) and the shift to 1715 cm^{-1} results from hydrogen bonding with urethane N−H groups.[61] For 3 wt % samples melt-blended and solvent-mixed, the intensity ratio between hydrogen-bonded and "free" carbonyl domain is not

(55) Brune, D. A.; Bicerano, J. *Polymer* **2001**, *43*, 369–387.
(56) Schaefer, D. W.; Justice, R. S. *Macromolecules* **2007**, *40*, 8501–8517.
(57) Gomez-Navarro, C.; Burghard, M.; Kern, K. *Nano Lett.* **2008**, *8*, 2045–2049.
(58) Lape, N. K.; Nuxoll, E. E.; Cussler, E. L. *J. Membr. Sci.* **2004**, *236*, 29–37.
(59) Bharadwaj, R. K. *Macromolecules* **2001**, *34*, 9189–9192.
(60) Forsyth, P. A., Jr.; Marcelja, S.; Mitchell, D. J.; Ninham, B. W. *Adv. Colloid Interface Sci.* **1978**, *9*, 37–60.
(61) Seymour, R. W.; Allegrezza, A. E.; Cooper, S. L. *Macromolecules* **1973**, *6*, 896–901.

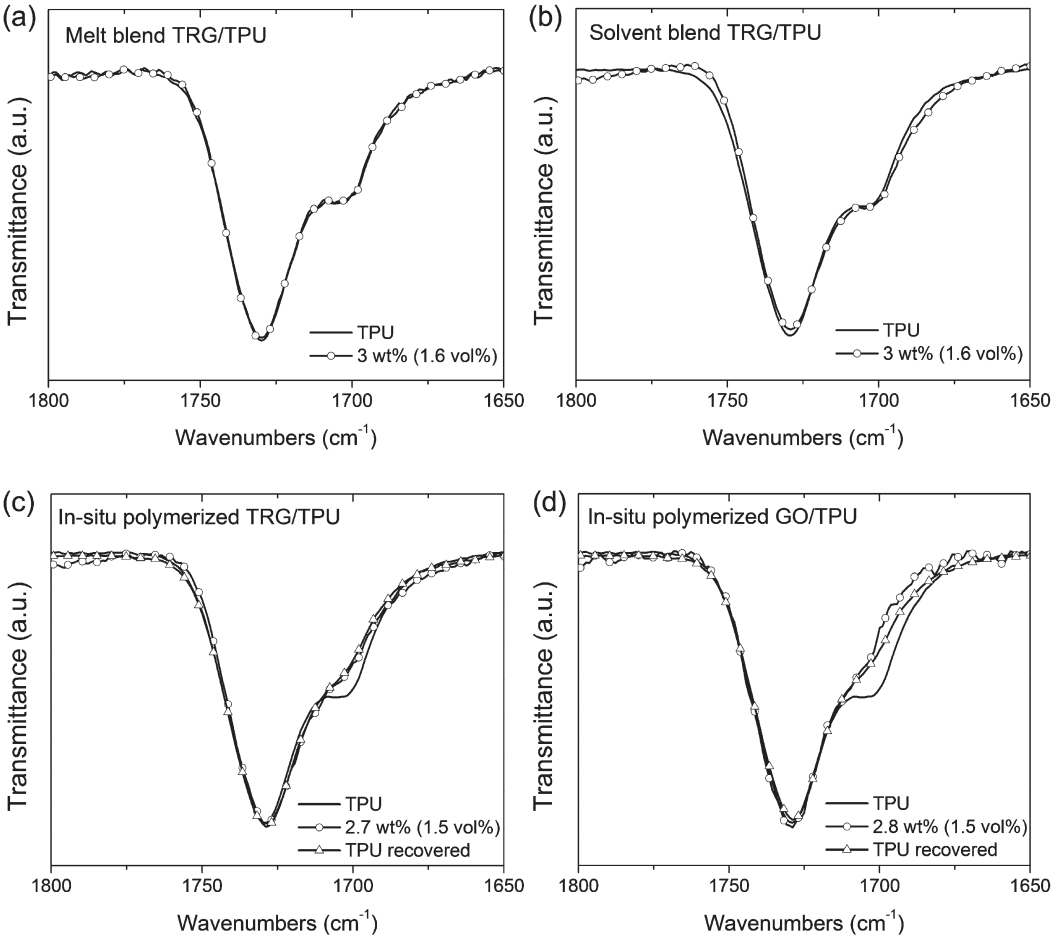

Figure 9. ATR FTIR spectra of (a) melt-blended, (b) solvent-blended, (c) in situ polymerized TRG, and (d) GO/TPU composites. For in situ polymerized samples, spectra of TPU recovered from the composites by Soxhlet extraction are also shown.

altered (Figure 9a,b). However, significant suppression in hydrogen bonding can be inferred from the diminished shoulder intensity at 1715 cm^{-1} for in situ polymerized TRG or GO composites (Figure 9c,d). Interestingly, TPU matrix extracted from the composites also displays some reduction in carbonyl hydrogen bonding, indicating that its hard segment length distribution is modified by particle addition during polymerization. TRG or GO was added after prepolymer synthesis, but before addition of the chain extender, BDO. Because surface hydroxyl and carboxylic acid functionalities may react with isocyanate in prepolymers and unreacted MDI,[24] chain extension by BDO will be less likely. This will prevent formation of longer hard segments that phase separate and produce hydrogen bonded domains more readily. Higher $T_{g,\ soft}$ and less modulus increase by the addition of TRG/GO above $T_{g,\ soft}$ confirm the inter-domain mixing in in situ polymerized TPU (see Supporting Information 6).

Despite limited hydrogen bonding in in situ polymerized composites, TRG with multiple −OH groups may serve as a pseudo chain extender substituting for the interurethane physical links. Figure 10 shows solvent-blended and in situ polymerized ~1.0 wt % (0.5 vol %) TRG/TPU films after 5 min and 24 h immersion in THF. A fraction of particulates maintaining the original shape implies only in situ polymerized TRG could not be completely extracted by THF in 24 h. Even intensive mechanical perturbation could not fracture the particle networks apart. TRG may form a sample spanning internal network that can self-sustain via chemical or physical cross-links mediated by grafted polymer chains. FTIR confirmed TPU grafting on functionalized graphene (Supporting Information 3) and dynamic mechanical analysis of in situ polymerized hybrids also substantiated existence of the network-like structure even at 0.5 wt % of TRG (Supporting Information 6).

4. Conclusions

In summary, graphite exfoliation can be achieved from GO via rapid thermal expansion (TRG) or surface treatments with isocyanate (iGO). Graphite, GO, and exfoliated graphene layers derived from GO were dispersed into TPU via melt compounding, solvent mixing, and in situ polymerization, the first time that these three dispersion methods have been compared. Solvent-based processes were more effective for obtaining well-distributed TRG throughout the matrix than melt processing as suggested by TEM and solid property enhancements. After solvent blending of TRG, TPU became electrically conductive at 0.5 wt %. With only 3 wt % of iGO or TRG, a 3- to 10-fold increase in tensile modulus and 80−90%

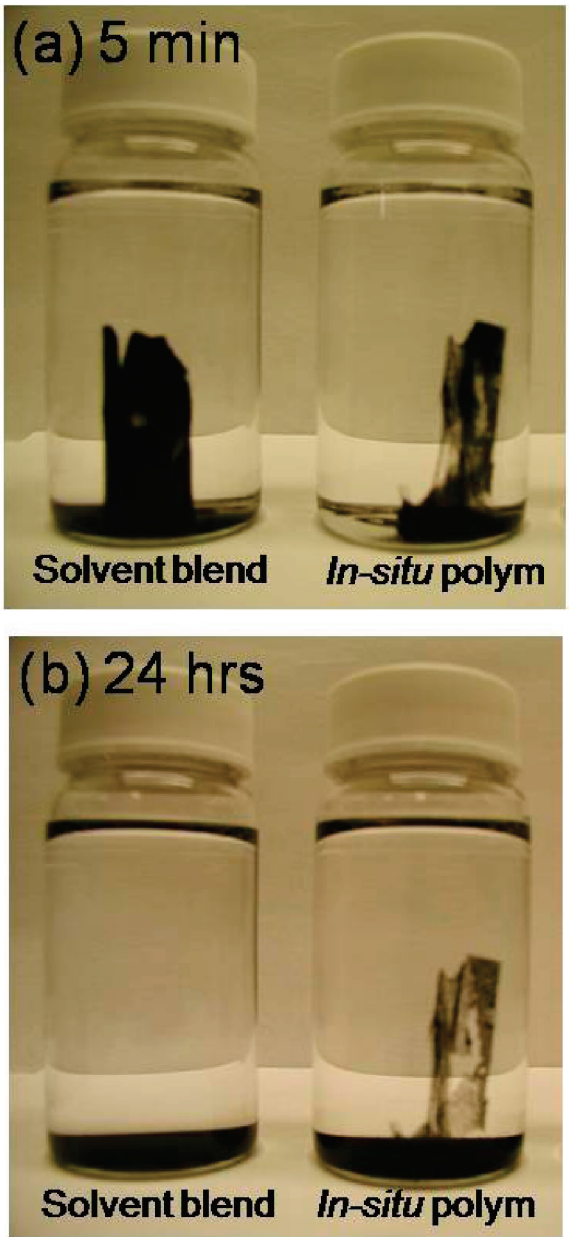

Figure 10. Solvent-mixed and in situ polymerized composite films containing ~0.5 vol % TRG immersed for (a) 5 min and (b) 24 h in 18 mL of THF.

reduction in N_2 permeability were attained. TRG dispersed by in situ polymerization formed strongly cross-linked networks, but also inhibited interchain hydrogen bonding in TPU matrix. This may account for less significant physical property gains for in situ polymerized composites than solvent-blended ones.

TRG is compatible with melt compounding and is as electrically conductive as unmodified graphite.[15] However, significant size reduction and structural distortion may reduce reinforcement efficiency of TRG for polymers. The large diameter of GO sheets can be preserved using chemical modification, which is beneficial for applications that require high aspect ratio of disklike particles such as gas barrier membranes. Strong interfacial bonding with matrix polymers enabled by surface functionalization is another advantage. Disadvantages include limitation in melt processing due to thermal instability and in situ chemical reduction steps required for electrical conductivity. Exfoliated carbon sheets can be better dispersed in polymers using solvent aided blending, thus enhance solid properties more effectively. Nonetheless, economical and environmental limitation makes the solvent-based processes less desirable. Although melt blending does not disperse particles as well, it can be done rapidly and economically with conventional polymer extrusion processes.

Acknowledgment. The authors appreciate Prof. Rodney S. Ruoff and Dr. Sasha Stankovich for their valuable comments on iGO synthesis. We also thank Prof. Robert K. Prud'homme at Princeton University, John Lettow and John Crain of Vorbeck Materials for providing TRG, Huntsman Polyurethanes for providing the TPU and materials for TPU synthesis, Prof. Michael Tsapatsis at the University of Minnesota for the gas permeation apparatus, Mingjun Yuan and Jeff Galloway at Entegris, Inc., for lending their surface resistance meter, and Prof. Ahmed A. Abdala at the Petroleum Institute (United Arab Emirates) for helpful input on the manuscript. We acknowledge financial support from the University of Minnesota Industrial Partnership for Research in Interfacial and Materials Engineering (IPRIME). Parts of this work were carried out in the University of Minnesota I. T. Characterization Facility, which receives partial support from NSF through the NNIN program, and in the Polymer Characterization Facility, which receives partial support from the NSF funded the University of Minnesota MRSEC.

Supporting Information Available: XPS, Raman, and FTIR spectra of graphitic derivatives; SEC traces of in situ polymerized composites; dynamic mechanical analysis and tensile test results of composite samples; and formulas and material parameters for mechanical property modeling (PDF). This material is available free of charge via the Internet at http://pubs.acs.org.